공학석사학위논문

Preparation and Characterization of Electrospun Conjugated Polymer Nanofibers with Controlled Diameter and Photovoltaics Thereof

전기방사를 이용하여 지름이 제어된 공액 고분자 나노섬유 제조 및 이에 기반한 태양전지 특성 분석

2012년 8월

서울대학교 대학원
재료공학부
김 성 균

Preparation and Characterization of Electrospun Conjugated Polymer Nanofibers with Controlled Diameter and Photovoltaics Thereof

전기방사를 이용하여 지름이 제어된 공액 고분자 나노섬유 제조 및 이에 기반한 태양전지 특성 분석

지도 교수 박 종 래

이 논문을 공학석사 학위논문으로 제출함

2012 년 5 월

서울대학교 대학원

재료공학부

김 성 균

김성균의 석사 학위논문을 인준함

2012 년 5 월

위 원 장	조 원 호	(인)
부위원장	박 종 래	(인)
위 원	장 지 영	(인)

Abstract

Preparation and Characterization of Electrospun Conjugated Polymer Nanofibers with Controlled Diameter and Photovoltaics Thereof

Kim, Sung-gyun

Department of Materials Science and Engineering

The Graduate School

Seoul National University

Organic photovoltaic (OPV) device is an energy conversion device which converts light into electricity. To improve the efficiency of the OPV, bulk heterojunction (BHJ) structured active layer is commonly used to increase the interfacial area between donor and acceptor, which cannot normally be accomplished in the bilayer structure. The extension of the interfacial area between donor and acceptor is expected to improve the exciton dissociation; thereby increasing the efficiency.

However, randomly orientated phases, which appear in the BHJ structured active layer, can result in unconnected islands and therefore reduce the charge transport efficiency. To improve the charge transport efficiency, continuous pathway should be fabricated in an active layer of BHJ OPV. For this purpose, electrospinning is utilized as a facile

method for the fabrication of 1-D conjugated polymer nanofibers.

For nanofibers with thinner diameter of nanofibers, a proper amount of PEO as an auxiliary polymer, along with DMF and acetic acid as polar solvents were added to the electrospinning dope solution. The addition of an auxiliary polymer increased the viscosity of the electrospinning dope solution and the addition of polar solvent increased the charge density of the electrospinning dope solution. Enhanced viscosity and enhanced charge density resulted in the fabrication of beadless, thin nanofibers.

After PEO, which is an insulator, was removed, thin P3HT nanofibers with a diameter of 80 nm was fabricated. In addition, the fabrication of PCDTBT nanofibers with a diameter of approximately 30 nm was accomplished by a similar method.

The exciton dissociation of the fabricated P3HT nanofibers was confirmed by photoluminescene quenching, which implies that the fiber can be utilized as an efficient OPV cell material. The power conversion efficiency of electrospun P3HT nanofiber-based OPV cells was c.a. 1 % and would be expected to be increased after the proper optimization processes.

Keywords: organic photovoltaic, conjugated polymer, electrospinning, nanofiber, exciton dissociation

Student Number: 2010-20581

Contents

List of Tables

List of Figures

1. Introduction

1.1 Organic photovoltaic cells

1.1.1 General introduction of OPVs

Solar cells are energy devices that absorb light and convert light into electricity. Solar cells are classified as inorganic solar cells or organic solar cell according to the type of materials in the active layer. Presently, inorganic silicon solar cells are most commonly used, and the Copper Indium Gallium Selenide (CIGS) inorganic solar cell shows high efficiency (~ 20%). However, the high production cost per unit and a lack of flexibility are the shortcomings of inorganic solar cells. In contrast, organic solar cells show low efficiency (~8%), but owing to advantages such as a low production cost, a light weight, and high flexibility, numerous recent studies have been carried out [1]. The device structure of an OPV is different from that of an inorganic photovoltaic cell. A typical solar cell consists of a cathode, an active layer, and an anode. For the cathode material, indium tin oxide (ITO) is generally used because ITO has high transparency of light on

transparent glass, high electrical conductivity, and a high work function which allows it to accept holes effectively. Aluminum (Al) is a typical anode material which has a low work function, allowing it to emit electrons well. The active layer is the core part of a solar cell. This layer absorbs light, generates excitons (pairs of holes and electrons), and transports electrons and holes to the anode and the cathode. The power conversion efficiency of an OPV is determined by its charge separation and transportation abilities. Charge separation and transportation depend on the morphology and structure of the active layer. Controlling the morphology and structure of the active layer is a critical factor when seeking to determine the power conversion efficiency of OPVs.

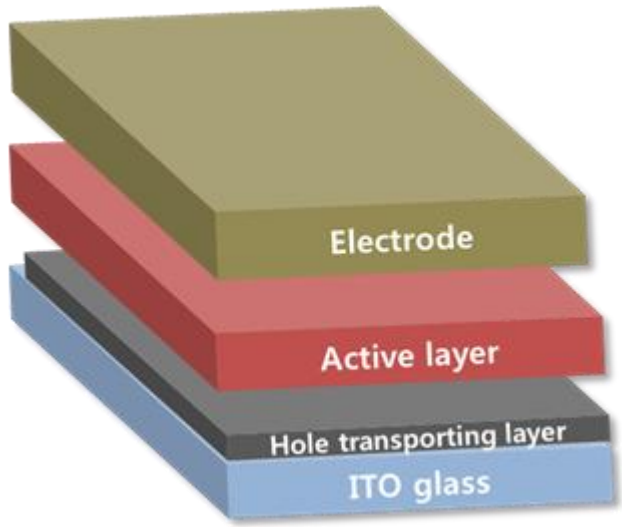

Figure 1.1 Sturcture of organic photovoltaic cells.

1.1.2 Operation principle and efficiency of OPVs

The charge generation mechanism of OPVs differs from that of silicon-based solar cells. The charge generation process in an OPV consists of three steps. First, the OPV absorbs light and generates excitons. Second, the excitons diffuse into the interface between the donor and the acceptor. Finally, the excitons are divided into holes and electrons and the holes and electrons are collected in the cathode and anode separately. To explain this in detail, once light is absorbed into the active layer, electrons in the donor material are excited and holes and electrons are then generated. At this time, the holes and electrons are bound by Coulombic force. This state is known as the exciton state. When excitons diffuse into the interface between the donor and acceptor, each of the excitons is separated by a gap between the HOMO (the highest occupied molecular orbital) energy level and the LUMO (the lowest unoccupied molecular orbital) energy level. The important point in this process is that the range of the diffusion length of an exciton in the organic active layer is approximately 10~20 nm [2-4]. If the distance between the exciton and the interface of the donor and acceptor is less than 10nm, the exciton can diffuse into the

interface sufficiently and be divided into an electron and a hole. However, if the distance is further than 10nm, the excitons are recombined and can no longer generate charges. Fig. 1.2 shows the process of exciton dissociation in the active layer of an OPV. After excitons are separated by electrons and holes, free holes move along the donor material to the cathode and free electrons move along the acceptor material to the anode.

The external quantum efficiency is defined by the formula shown in Fig. 1.3. Here, η_a is the absorption efficiency of the donor material, η_{ED} is the exciton diffusion efficiency, η_{CT} is the charge transfer efficiency, and η_{CC} is the charge collection efficiency [5]. According to this equation the external quantum efficiency of OPVs is determined by the photon absorption, exciton diffusion and separation, charge transport and collection. The power conversion efficiency of OPVs can be enhanced when each parameter, η_a, η_{ED}, η_{CT}, and η_{CC}, increases.

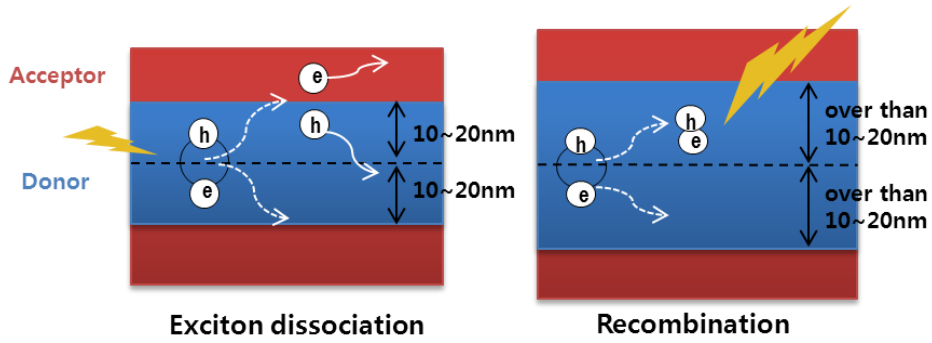

Figure 1.2 A schematic representation of exciton dissociation in active layer.

$$\eta_{EQE} = \eta_A * \eta_{ED} * \eta_{CT} * \eta_{CC}$$

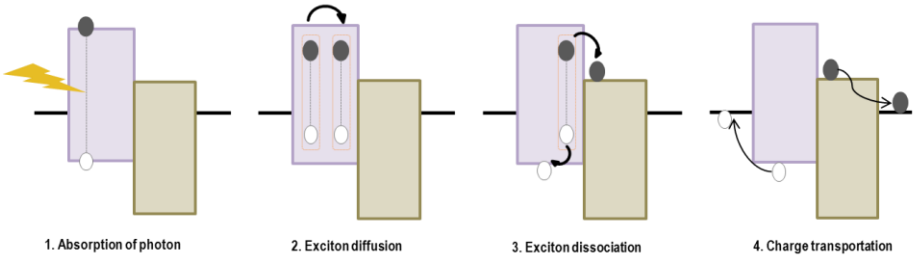

Figure 1.3 A schematic representation of external quantum efficiency.

1.1.3 Structure of active layer

The structure of the active layer is classified into two major types. The first type is a bilayer structure, like the inorganic photovoltaic cell, and the second structure is a bulk heterojunction structure. Tang announced that for the first time, he created a bilayer structure of an OPV with 1% efficiency in 1986 [6]. At this time, photovoltaic cells were fabricated by vacuum evaporation and the donor and acceptor materials were divided into separate layer. However, an OPV with a bilayer structure is limited in terms of its generation of holes and electrons because the exciton diffusion length is shorter than 10nm due to the extremely short time (100 ps) required for recombinations of holes and electrons into excitons and due to the area limit of the interface between the donor and acceptor [7, 8]. To overcome these limitations, a bulk heterojunction structure with an appropriately mixed active layer of the donor and acceptor has been investigated [9]. Specifically, in 1995 Heeger's group implemented a bulk heterojunction structure by means of a solution process, which is an easier method for organic materials compared to vacuum evaporation.

They found that a bulk heterojunction structure makes exciton dissociation more effective, which enhances the efficiency of the OPV [10]. In 2005, Heeger and Carroll fabricated a bulk heterojunction OPV with P3HT, which is a typical donor material. This cell showed 5% efficiency. Currently, OPVs commonly adopt a bulk heterojunction structure [11].

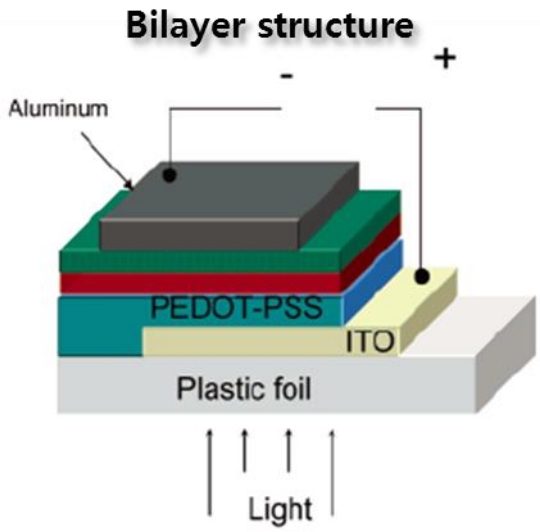

Figure 1.4 A schematic representation of bilayer structured OPV cell [9].

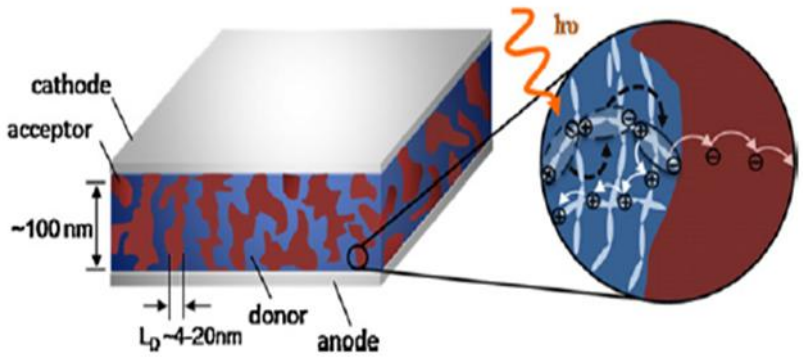

Figure 1.5 A schematic representation of bulk heterojuction structured OPV cell [12].

However, the bulk heterojunction structure has some disadvantages. To make a bulk heterojunction structure, the donor materials and acceptor materials are normally mixed and spin-coated onto the substrate. This method enlarges the surface area of the interface between the donor and acceptor, but it also creates isolated domains due to the random distribution and orientation of the materials. Figure 1.6 shows a TEM image of the active layer, showing that some domains are isolated while most of the white donor phase and black acceptor phase are well mixed. Although the excitons are successfully divided and generate holes and electrodes effectively, in the isolated domains, divided charges cannot move between electrodes, and electron and hole recombine. This limits the enhancement of the efficiency of an OPV. Therefore, adopting a continuous pathway in the donor and acceptor phase in the active layer is necessary to circumvent the limits of the bulk heterojunction structure [13].

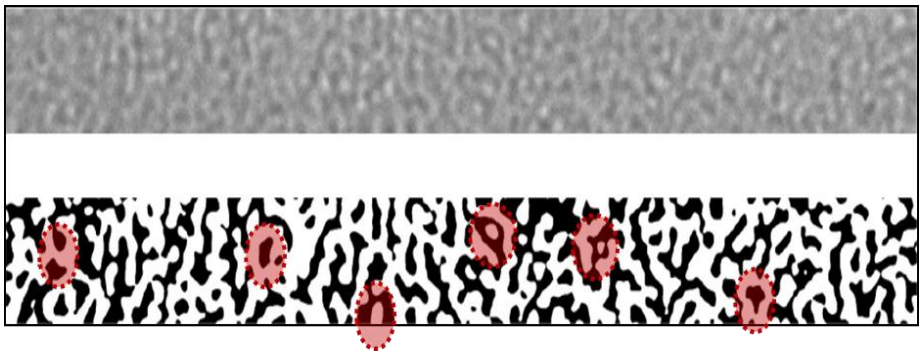

Figure 1.6 Focused cross-sectional TEM image (upper imager) and corresponding binary image (lower image) and isolated domains (red circle) [14].

1.2 1-D conjugated polymer

1.2.1 Advantages of 1-D conjugated polymer

One-dimensional (1-D) materials with a high aspect ratio are known to be useful for building effective charge transport pathways due to their low percolation threshold [14,15]. Moreover the electrical properties of 1-D conjugated polymer are better than those conjugated polymer film, meaning that, for example, poly(3-hexylthiophene) (P3HT) nanorods are expected to form effective charge transport pathways while also providing a higher charge mobility than P3HT films [16], thus enabling the preparation of high efficiency OPV cells [17].

1.2.2 Fabrication of 1-D conjugated polymer

1.2.2.1 Merits and demerits of fabrication method

During the last few decades, the fabrication of 1-D conjugated

polymers has been widely studied. As a result, various techniques such as nanoimprint lithography [18], different templating methods [16] and self-assembly processes [19] have been proposed. However, covering a large area with 1-D conjugated polymers is not easy because the first two methods are intrinsically limited in scale while the third method has only been applied to P3HT of known conjugated polymers owing to the variability of the self-assembly behaviors of such materials [20]. Moreover, in the first and second methods, this process includes making a template and transferring the 1-D material, meaning that it is not a straightforward process. Therefore, when using the first two methods, it is necessary to make the template and transfer a 1-D array onto the substrate, making this a rather complicated process. In contrast, the electrospinning technique is comparatively simple and convenient for fabricating 1-D forms of various materials over a large area [21]. This technique has an additional advantage over spin-coating, which has conventionally been the technique of choice for OPV cell fabrication: the higher throughput obtained with a multi-nozzle and the less waste of materials [22, 23].

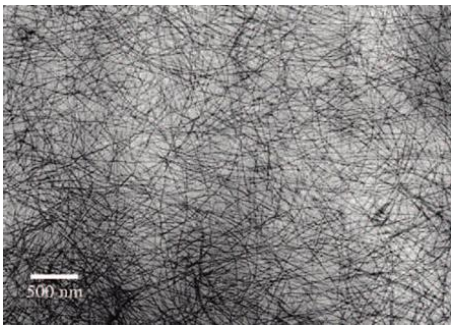

(a)

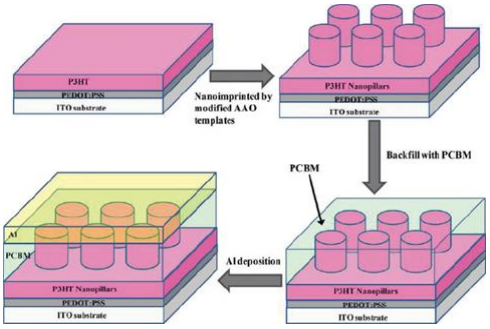

(b)

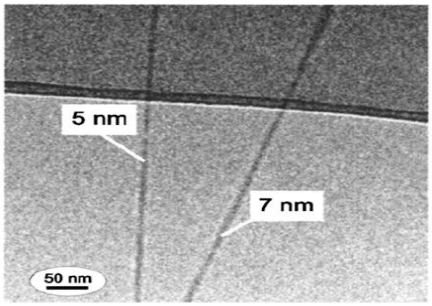

(c)

Figure 1.7 Various 1-D conjugated polymer fabrication method (a) Self-assembly [19] , (b) Nanoimprint lithopgraphy [18], (c) Electrospinning [24].

1.2.2.2 Electrospinning

Electrospinning gives the impression of being a very simple and, therefore, easily controlled technique for the production of fibers with dimensions down to the nanometer range. In a typical electrospinning experiment in a laboratory, a polymer solution or melt is pumped through a thin nozzle with an inner diameter on the order of 100 mm. The nozzle simultaneously serves as an electrode, to which a high electric field of 100–.500 kVm1 is applied, and the distance to the counter electrode is 10–.25 cm in laboratory systems. The substrate onto which the electrospun fibers are collected is typically brought into contact with the counter electrode.

The applied voltage causes a cone-shaped deformation of the drop of polymer solution, in the direction of the counter [24, 25]. In the electrospinning process, if higher voltages are applied, a jet is formed from the deformed drop, which moves towards the counter electrode and becomes narrower in the process [26, 27]. On the way to the counter electrode, the solvent evaporates (or the melt solidifies), and solid fibers with diameters ranging from micrometers to nanometers are precipitated with high velocities on the counter electrode. The

shapes and dimensions of the fibers formed depend on a large set of parameters, for example, the properties of the polymer itself (such as the molecular weight, molecular-weight distribution, glass-transition temperature, and solubility), as well the properties of the polymer solution (such as the viscosity, viscoelasticity, concentration, surface tension, and electrical conductivity). The vapor pressure of the solvent and the relative humidity of the surroundings can also have a significant impact.

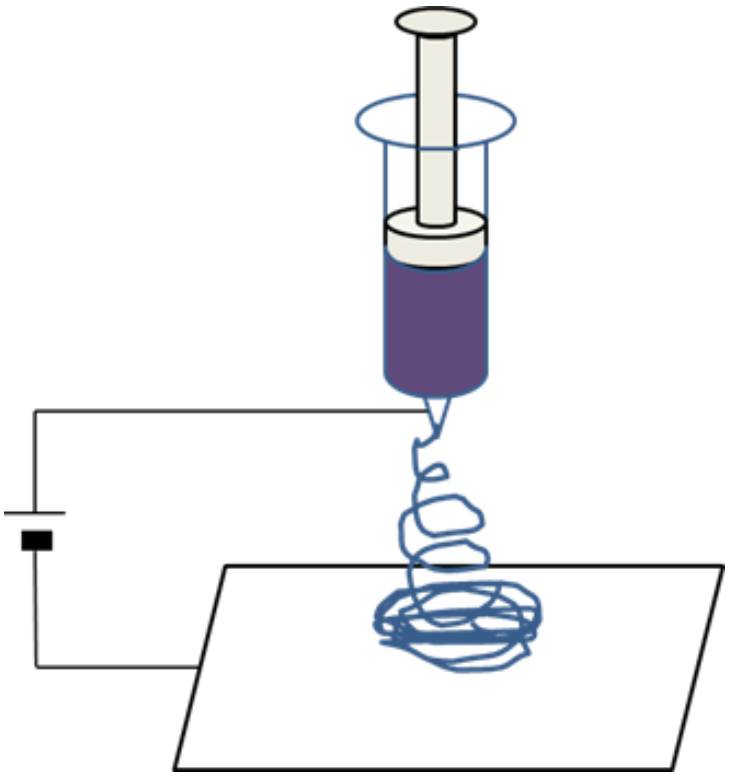

Figure 1.8 A schematic representation of electrospinning.

1.3 State of the art of electrospun 1-D conjugated polymer

1.3.1 Conventional electrospun P3HT fibers

P3HT is the most well-known conjugated polymer used as a donor material for OPVs. Figure 1.9 shows studies related to P3HT nanofibers fabricated by the electrospinning method. P3HT nanofibers were electrospun with only chloroform in Figure 1.9 (a), with auxiliary polymer and chloroform in Figure 1.9 (b), (d), with dual nozzle system in Figure 1.9 (c).

1.3.2 Difficulty of electrospun P3HT fiber with small diameter

However, to the best of our knowledge electrospun conjugated polymer fibers have never been used for the fabrication of OPV cells. The fiber diameter should be as small as possible in order to produce an effective exciton diffusion length; the generated electron–hole pairs will soon be annihilated by recombination during diffusion through fibers with large diameters. It is however not easy to prepare homogeneous conjugated polymer nanofibers of diameters below 100

nm through electrospinning.

There are several reasons for these difficulties. Firstly, conjugated polymer solutions usually have viscosities that are too low for electrospinning, and thus many beads form on the fibers due to Rayleigh instability [28]. When a high concentration of conjugated polymer is used to provide high viscosity, the nozzle frequently becomes clogged because the usual solvent for conjugated polymers, i.e., chloroform, evaporates very quickly, and a large amount of conjugated polymer accumulates on the tip of the nozzle. This precipitation of polymer results in the formation of inhomogeneous nanofibers. Some other nonvolatile solvents for conjugated polymers, such as dichlorobenzene and toluene, can be used instead of chloroform but these solutions do not evaporate completely during the electrospinning process. The use of auxiliary polymers such as poly (methyl methacrylate) (PMMA) and poly (ethylene oxide) (PEO) has been suggested with the aim of increasing the viscosity of the electrospun doping solution [29, 30]. Indeed, the use of an auxiliary polymer does make it possible to use electrospinning solutions containing low concentrations of conjugated polymers, which prevents clogging. Secondly, because the dielectric constant and conductivity

of solvents for conjugated polymers are low, the diameters of the resulting fibers are still on the order of hundreds of nanometers, even when electrospinning without clogging is achieved through the use of an auxiliary polymer [29, 30]. To obtain thin nanofibers, the solvent used in the spinning of a doped preparation should have a high dielectric constant and high electric conductivity, as is the case for most polar solvents. Thin nanofibers can then be achieved for the following reasons: firstly, the high charge density of the solution hampers the formation of beads due to the electric repulsion force, which means that solutions of low concentrations can be electrospun to produce thin nanofibers fabricated by an electrospinning method [31].

Secondly, the high charge density of the solution generates bending instability more easily; thus, a whipping cloud forms closer to the nozzle tip, which remarkably increases the flight distance [32]. A long flight distance means that the solution is stretched more, which leads to fibers with reduced diameters. However, most conjugated polymers do not dissolve in polar solvents. Therefore, ultrathin conjugated polymer nanofibers, i.e., with diameters below 100 nm, cannot be obtained. There have been a few previous reports of conjugated

polymer fibers with diameters below 100 nm achieved by electrospinning with a dual nozzle system [33, 34], but this approach requires a somewhat complicated set-up and complex spinning conditions.

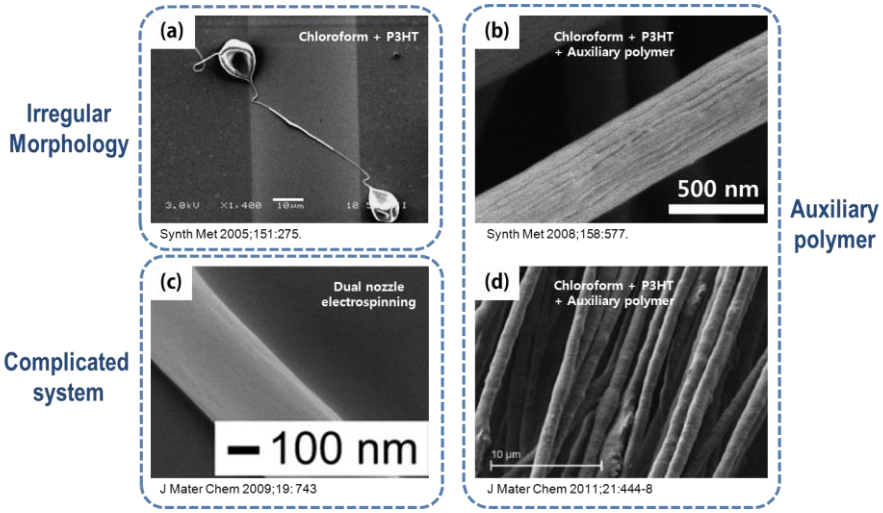

Figure 1.9 Scanning electron micrographs of electrospun P3HT fiber using (a) chloroform + P3HT [35], (b) (d) additive of auxiliary polymer [36, 37], (c) dual nozzle system [38].

1.4 Objective of present work

So that an OPV can absorb light and produces light, the OPV should generate excitons easily in the active layer and should transfer holes and electrons to the electrodes efficiently. To accomplish effective exciton dissociation, the domain size should be within 10nm. To collect holes and electrons without recombinations, donor and acceptor materials should form a continuous pathway. In this research, to obtain conjugated polymer nanofibers with diameters of ~20nm, an electrospinning method with the merit of being able to create a 1-D structure material should be used. To fabricate a nanofiber with a narrow diameter, a specific co-solvent and an auxiliary polymer were added here to the electrospun doping solution. By controlling the conductivity and viscosity with this process, the possibility of narrowing the diameter of the nanofiber was assessed. Meanwhile, to verify whether this method can be adopted with various conjugated polymers for OPVs, in addition to P3HT, a well-known donor material with an electrospinning method was used with MDMO-PPV and PCDTBT and nanofibers were fabricated. In particular, with P3HT, to

check its feasibility as active layer on an OPV, various measurements were conducted. First, after eliminating the auxiliary polymer, which has an insulating property, PCBT was coated onto the P3HT nanofibers. The exciton dissociation was then checked by measuring the PL performance. Also, by fabricating an OPV cell with P3HT nanofibers, the actual performance of the OPV was measured.

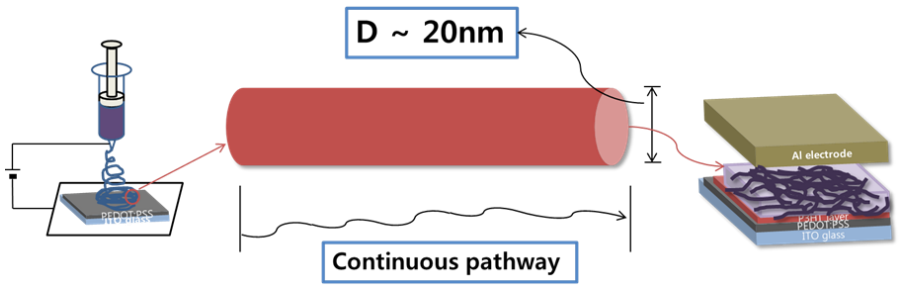

Figure 1.10 A schematic representation of cell fabrication process

2. Experimental

2.1 Chemicals and materials

P3HT (Mw 50,000; Rieke metal), PEO (Mw 900,000; Aldrich), Poly[2-methoxy-5-(3′,7′-dimethyloctyloxy)-1,4-phenylenevinylene] (MDMO-PPV; Mn 23,000; Aldrich), Poly[N-9'-heptadecanyl-2,7-carbazole-alt-5,5-(4',7'-di-2-thienyl-2',1',3'-benzothiadiazole)] PCDTBT; Mw 82,200; Osilia), PCBM (Nano-C), chloroform (Aldrich), acetic acid (Aldrich), *N,N'*-dimethylformamide (DMF; Daejung, Korea), acetonitrile (Aldrich), and dichloromethane (Aldrich) were purchased and used without further purification.

2.2 Electrospinning of conjugated polymer nanofiber

To prepare the electrospinning dope solution, specified amounts of PEO, the auxiliary polymer, and conjugated polymer were dissolved either separately or together in chloroform with stirring at 50 ˚C for 6

h. The solutions were electrospun either as prepared or after mixing with various amounts of a polar cosolvent composed of 2 mol of acetic acid and 1 mol of DMF. The compositions of the solutions are specified below in weight percent with respect to the weight of the solvent.

The electrospinning dope solution was loaded into a syringe connected to a metal needle (gauge no. 28, inner diameter 0.18 mm) nozzle and electrospun at a feeding rate of 1.0 mL/h in air at 25~26 ˚C and 19~21% relative humidity, a bias voltage of 23 kV was applied to the metal needle, and the distance from the nozzle to the grounded collector plate was approximately 21 cm. For uniform electrospinning, the collector glass plate and the needle nozzle were reciprocated by a 3-axis robot. The as-spun composite nanofibers were subjected several times to acetonitrile for 30 min to remove PEO and finally P3HT nanofibers were obtained.

2.3 Fabrication of electrospun nanofiber based OPVs

ITO-coated glass (15 Ω/sq) was cleaned with distilled water, acetone and isopropyl alcohol, and then treated with UV–ozone for 5 min. PEDOT:PSS was spin coated at 4000 rpm, and the PEDOT:PSS film was annealed at 150 °C for 5 min. P3HT buffer layer was prepared by spin coating (a spin rate of 3000 rpm) P3HT solution (5 mg P3HT in 1 mL chlorobenzene). P3HT nanofibers were electrospun onto the P3HT buffer layer using abovementioned condition. After removal of auxiliary polymer, PCBM layer was spin-cast (a spin rate of 600 rpm) from PCBM solution (20 mg PCBM in 1 mL dichloromethane) onto a glass plate covered with P3HT nanofibers. Al electrode was thermally evaporated on the top of the active layer under vacuum lower than 10^{-6} Torr. The devices were then thermally annealed at 150 °C inside the glove box.

2.4 Characterization

The morphologies of the composite nanofibers and the P3HT nanofibers were examined under a field emission scanning electron microscope (FESEM; JEOL JSM-6700F) operating at an accelerating voltage of 5 kV. The conductivity of each spinning dope solution was measured with an Orion 4-Star pH-Conductivity Meter (Thermo Fisher Scientific Inc.). Thermogravimetric analysis (TGA) was carried out under nitrogen flow with a heating rate of 10 ˚C /min and isothermal processing at 370 ˚C for 30 min by using an SDT Q 600 instrument (TA Instruments). The X-ray diffractograms of the P3HT nanofibers were recorded in reflection mode, which is standard procedure for X-ray diffraction measurements, by using Ni-filtered Cu Kα radiation (λ_f = 0.154184 nm) on a D8-Advance diffractometer (Bruker). For comparison, P3HT spin-coated on a silicon wafer was also subjected to X-ray diffractometry. The thickness of the spin-cast film was found to correspond to the amount of electrospun P3HT.

The ultraviolet-visible absorption characteristics of a sample prepared by spin-coating 1 wt% P3HT solution in chloroform onto a glass substrate at 600 rpm were examined by using a Cary 5000

(Varian Inc.). The photoluminescence properties were examined at the excitation wavelength of 470 nm on an LS-55 (Perkin-Elmer). The current density-voltage (J–V) characteristics were measured with a K3000 (McScience) under AM 1.5 G (100mW/cm^2).

3. Results and discussion

3.1 Effects of additives in electrospinning dope solution

3.1.1 Effects of auxiliary polymer (PEO)

Auxiliary polymers such as PVP, PMA, and PEO are used to prepare electrospun fibers. Among the many auxiliary polymers available at present, PEO is used because it is readily dissolved in chloroform, which can dissolve many conjugated polymers, including P3HT. Due to its high molecular weight, the viscosity of the dissolved solution is greatly increased only with a small amount of PEO. With the same charge density, if the viscosity of an electrospun doping solution increases, long fibers are readily created because the electrospinning dopw solution has both well-entangled polymers and a solvent. As shown in Figure 3.1, whereas the P3HT/chloroform solution without PEO was electro-sprayed due to a lack of viscosity, the addition of PEO into the P3HT/chloroform solution resulted in viscosity high enough to make electrospun nanofibers with a high

aspect ratio. Figure 3.2 shows that the viscosity of the solution is increased as the PEO concentration (wt %) in the electrospinning dope solution increases.

Although PEO helps to increase the viscosity of electrospinning dope solution, added PEO can act as an insulator and can become excessively entangled to make beads, even causing the nozzle to become clogged.

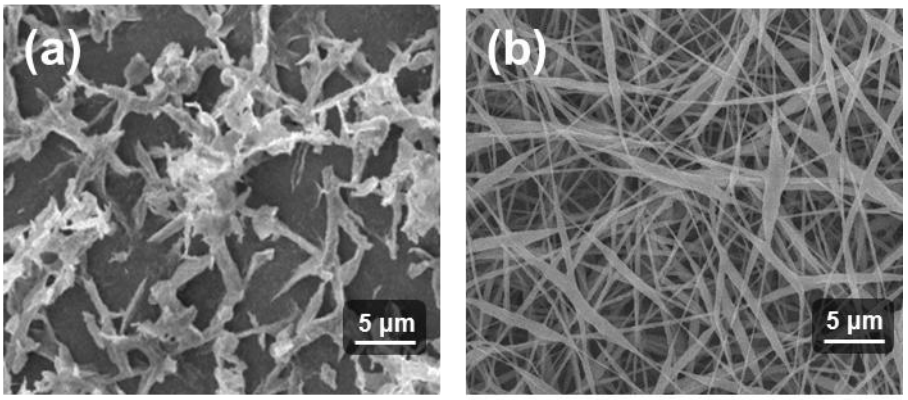

Figure 3.1 Scanning electron micrographs of nanofibers from (a) P3HT 1wt% solution and (b) P3HT 1wt% and PEO 1wt% solution .

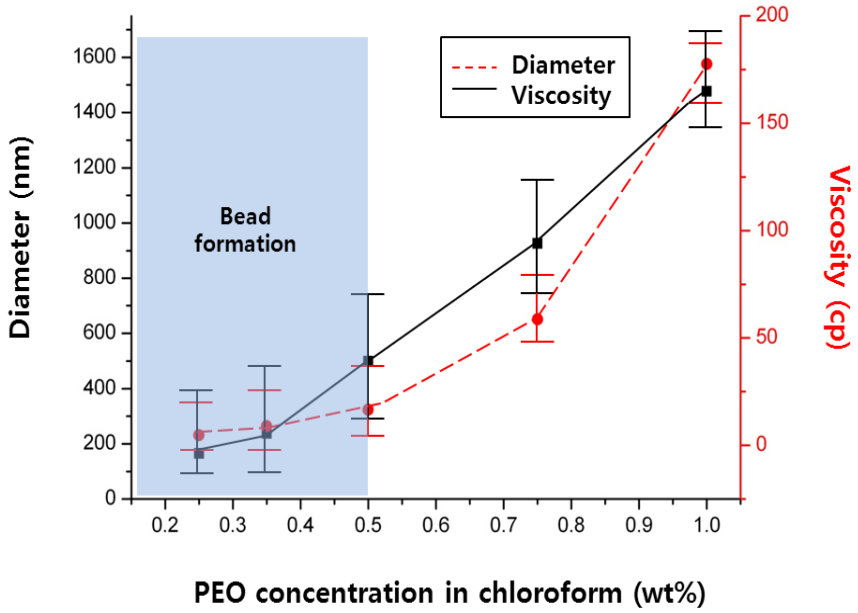

Figure 3.2 The variations in the viscosity of the electrospinning dope solution and the diameter of the electrospun PEO nanofibers.

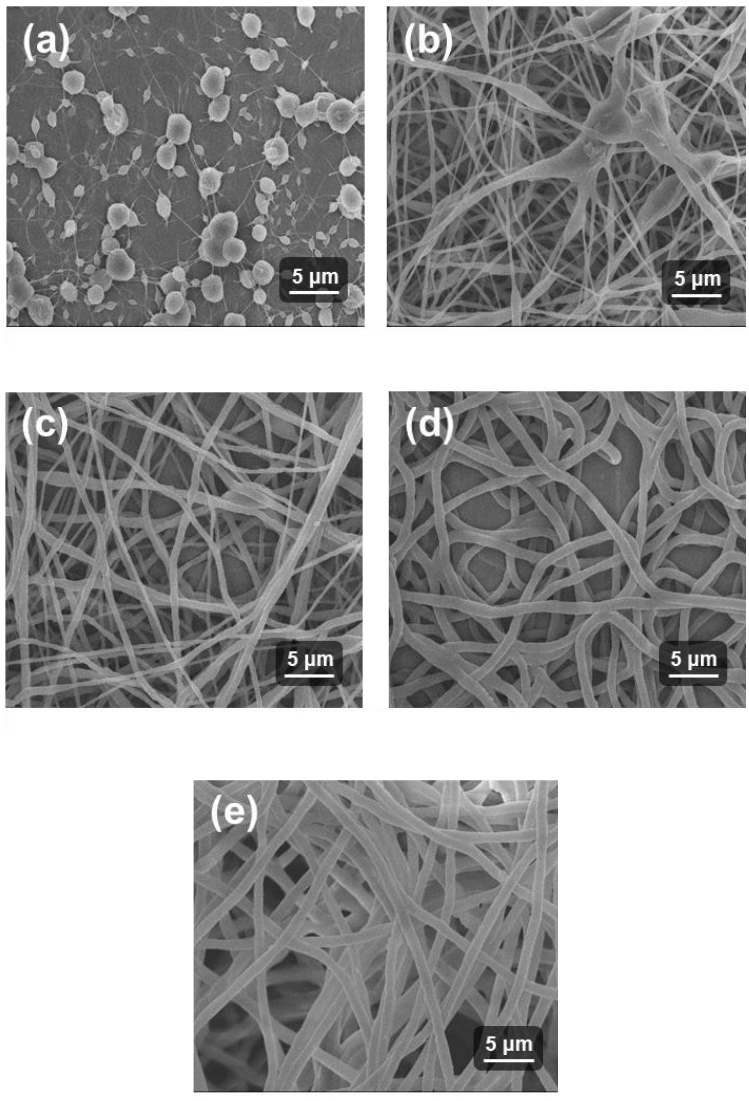

Figure 3.3 Scanning electron micrographs of electrospun PEO nanofibers with various concentration of PEO (a) 0.25wt%, (b) 0.35wt%, (c) 0.5wt%, (d) 0.75wt%, (e) 1 wt%.

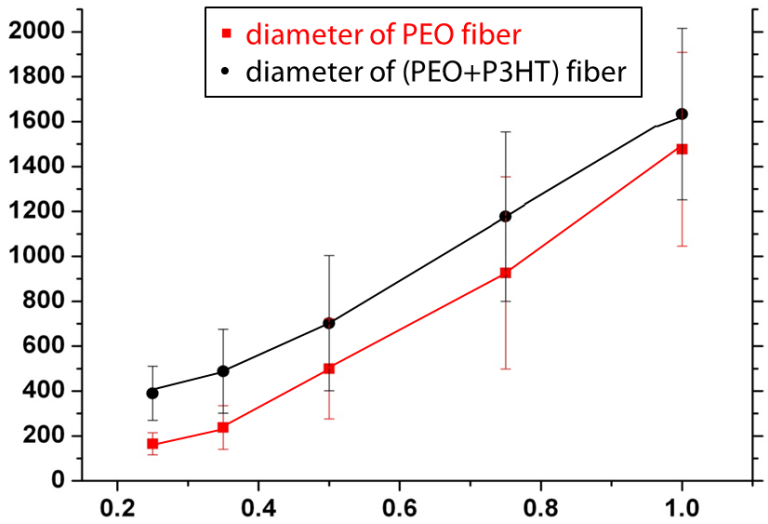

Figure 3.4 The variations in the diameter of the electrospun (PEO+P3HT) nanofibers [39].

In particular, because an increase in the amount of PEO results in nanofibers with large diameters, the amount of added PEO should be controlled in order to make long nanofibers without beads. To investigate the optimum viscosity value which can be achieved with the minimum amount of PEO, different concentrations of PEO in chloroform were tested until beads were not formed. As shown in Figure 3.2, both the viscosity and diameter of the nanofibers increase as the PEO wt% concentration increases. Fibers with less than 0.5 wt% of PEO have insufficient viscosity to form beads (Figure 3.2). Compared to the case with PEO only, when P3HT and PEO were used, the diameter of the nanofibers increased more due to the addition of P3HT. However, the overall increasing tendency of the diameter and the viscosity as a function of the PEO wt% concentration is analogous to those results for the PEO-only case. It was validated that PEO plays a major role in electrospinning. Therefore, according to the above results, in the experiment, the PEO wt% concentration was fixed at 0.5 wt% to reduce the formation of beads and obtain a sufficient viscosity with minimal use of the insulation material, PEO. However, as shown in Figure 3.3, the minimum diameter of electrospun P3HT nanofibers with 0.5 wt% PEO was approximately 500 nm. This size was longer

than the exciton diffusion length in the conjugated polymer. As a result, for efficient exciton dissociation, the diameter of the nanofibers should be held to a smaller value.

3.1.2 Effects of polar solvent

Although P3HT nanofibers can be made by adding an auxiliary polymer (PEO) to the electrospinning dope solution, the diameter of the resulting nanofibers is larger than 500 nm, even after removing the insulating PEO. To decrease the diameter of the nanofibers further, a polar solvent, e.g., DMF, acetic acid, distilled water, or ethanol should be used. Among the commonly used polar solvents for electrospinning, DMF and acetic acid were used due to their high electrical conductivity. In addition, DMF has a high dielectric constant, and acetic acid can be used to complement the poor viscosity of DMF. Adding DMF and acetic acid increases the charge density of the solution, which increases the electrostatic repulsion force. This prevents the formation of beads and makes nanofibers more instable. As a result, a whipping cloud forms near the electrospinning nozzle,

and thinner and longer nanofibers can be formed according to the increased flight distance. As shown in Figure 3.7, when the polar solvent was added to the electrospun doping solution, a decrease in the diameter of the fiber to approximately 100 nm was noted. The diameter of the fiber linearly depends on the concentration of the polar solvent (Figure 3.6); however, a large amount of polar solvent can decrease the viscosity of the electrospun doping solution, leading to the creation of beads. Moreover, because the auxiliary polymer, PEO, has low dissolution affinity with DMF, the optimum concentration of the polar solvent should be identified. With a fixed optimum concentration of PEO and chloroform, different concentrations of polar solvent were added to make electrospun fibers. The optimum concentration of the polar solvent was tested without P3HT because PEO plays a strongly dominant role in the electrospinning process. The optimum concentration of the polar solvent is 12 – 13 wt% and the thinnest P3HT/PEO nanofibers with a 100 nm diameter were obtained under this condition.

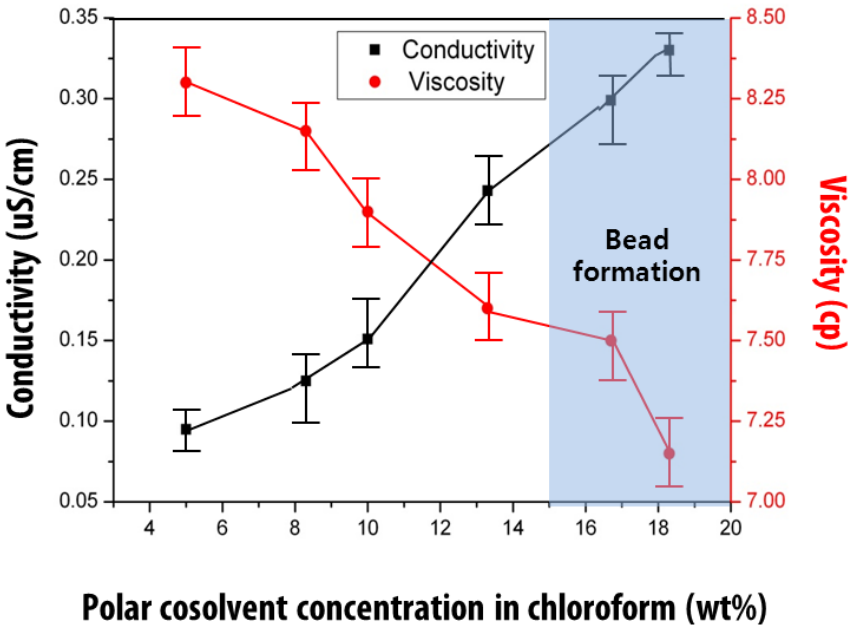

Figure 3.5 The variations in the conductivity [39] and viscosity of the electrospinning dope solution of electrpsun P3HT nanofiber.

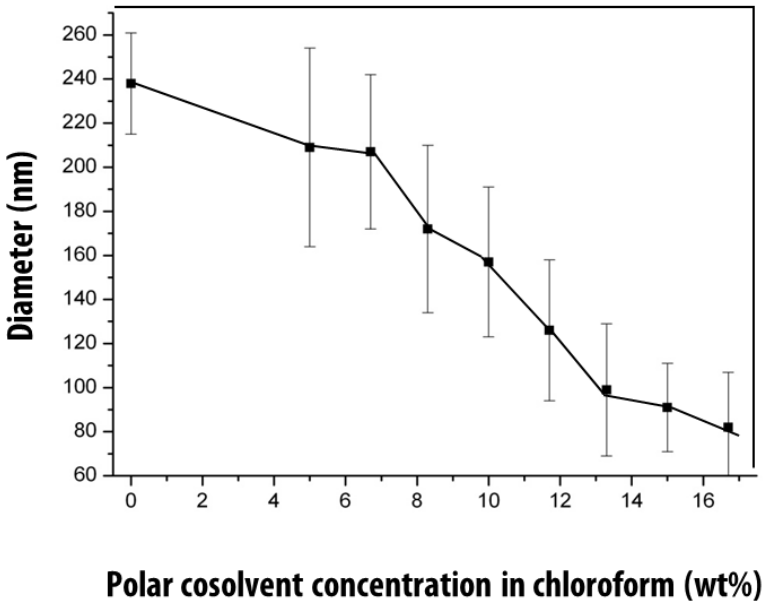

Figure 3.6 The variations in the the diameter of the electrospun PEO nanofibers.

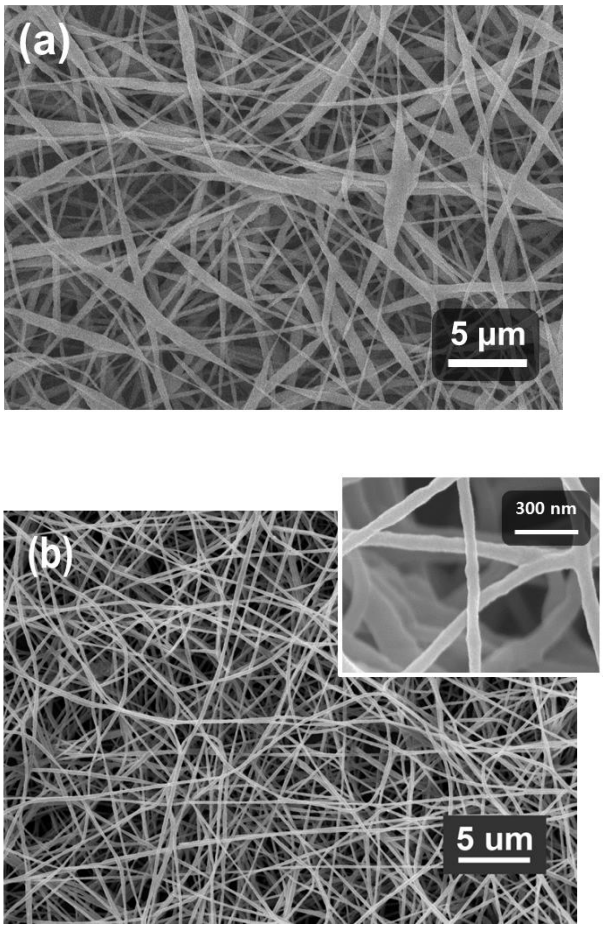

Figure 3.7 Scanning electron micrographs of electrospun P3HT/PEO nanofibers (a) without polar solvents (b) with polar solvents (inset: a magnified image).

3.2 Fabrication of conjugated polymer nanofibers with small diameter

3.2.1 Electrospun conjugated polymer nanofibers

Recently, in addition to P3HT as a typical polymer donor material for OPVs, various conjugated polymers have also been developed. In addition, the reported cell efficiency of OPVs based on these materials is superior to that based on P3HT. To confirm the applicability of this method to other conjugated polymers which previously achieved a thin 80nm diameter of the P3HT nanofibers, electrospun nanofibers of MDMO-PPV and PCDTBT were manufactured. As illustrated in Figure 3.8, the MDMO-PPV sample was slightly thicker than the P3HT sample. However, overall the nanofibers were equal in terms of their diameters. Especially in the case of PCD-TBT, it showed a diameter nearly identical to or thinner than that of P3HT.

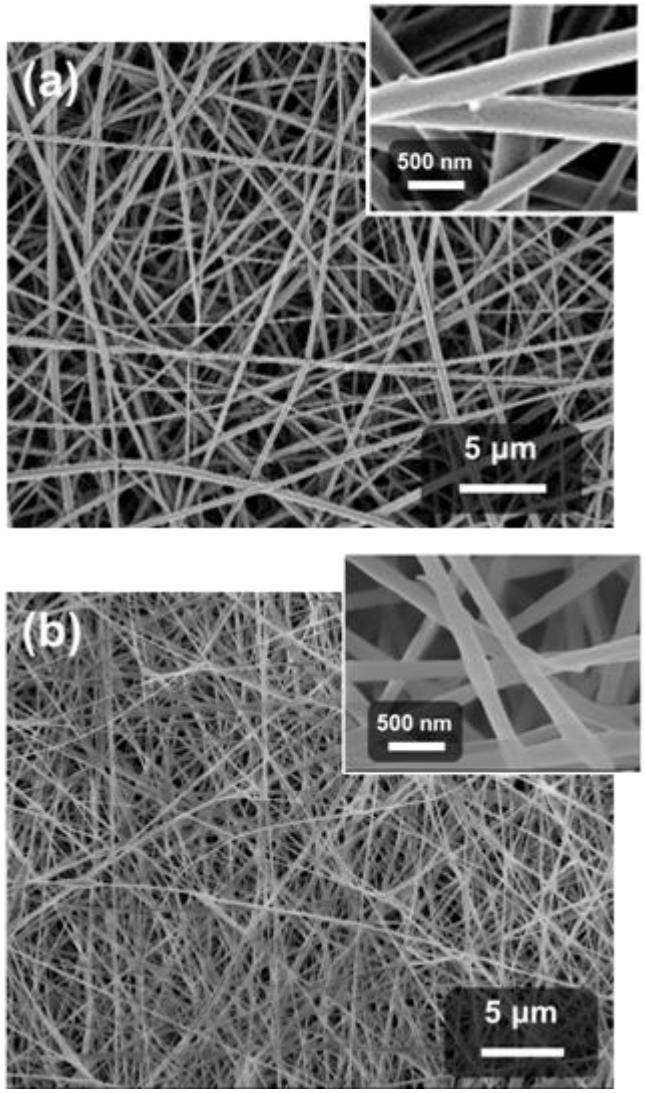

Figure 3.8 Scanning electron micrographs of electrospun nanofibers (a) MDMO-PPV/PEO with polar solvent (b) PCDTBT/PEO with polar solvent.

3.2.2 Removal of auxiliary polymer (PEO)

In order to use the electrospun P3HT/PEO nanofibers as a donor substance on an active layer, the insulating PEO should be eliminated by dipping the nanofibers into acetonitrile. A thermogravimetric analysis (TGA) was conducted in a further investigation of the removal of PEO; while all of the PEO was decomposed, P3HT did not show any apparent change under a nitrogen flow at 370℃ for 30 min. After the PEO was removed, the measured amount of P3HT residue via TGA under the same condition is similar to that of the theoretically calculated value of P3HT residue. Figure 3.9 shows the amount of PEO residue as a function of the number of dips into the acetonitrile. When the fiber was dipped into acetonitrile once, the PEO residue remained at about 17 % of its pristine weight. After a second dipping, the PEO residue was decreased to 2-3 wt%, and this weight was maintained even after more than three dips. Therefore, the number of dips should be more than two in order to remove the PEO. From micrographs of the fibers, the continuous morphology of nanofibers was well maintained before and after the removal of the PEO. In particular, the TEM image shows that the diameter of the P3HT

nanofibers decreased by as much as 80 nm (Figure 3.10)

After the PEO elimination process, the shape of the nanofibers was maintained in both polymers. The diameter of the PCDTBT nanofibers was close to 30nm. This diameter size is close to the nanofibers diameter target of ~20nm, which was set considering the exciton diffusion length.(Figure 3.11)

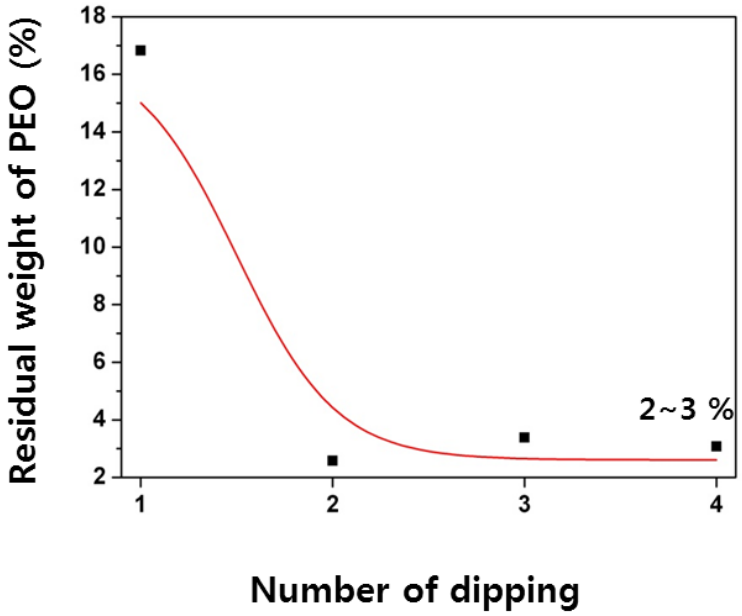

Figure 3.9 The residual weight of PEO in P3HT electrospun nanofiber after dipping in acetonitrile.

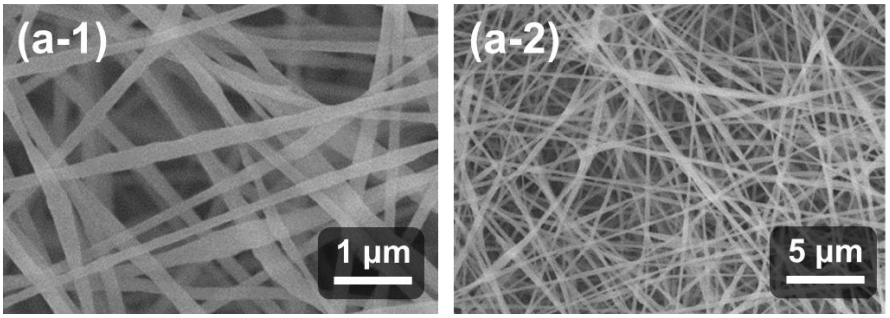

Figure 3.10 Scanning electron micrographs of electrospun P3HT fibers before (a) and after (b) [39] removal of auxiliary polymers.

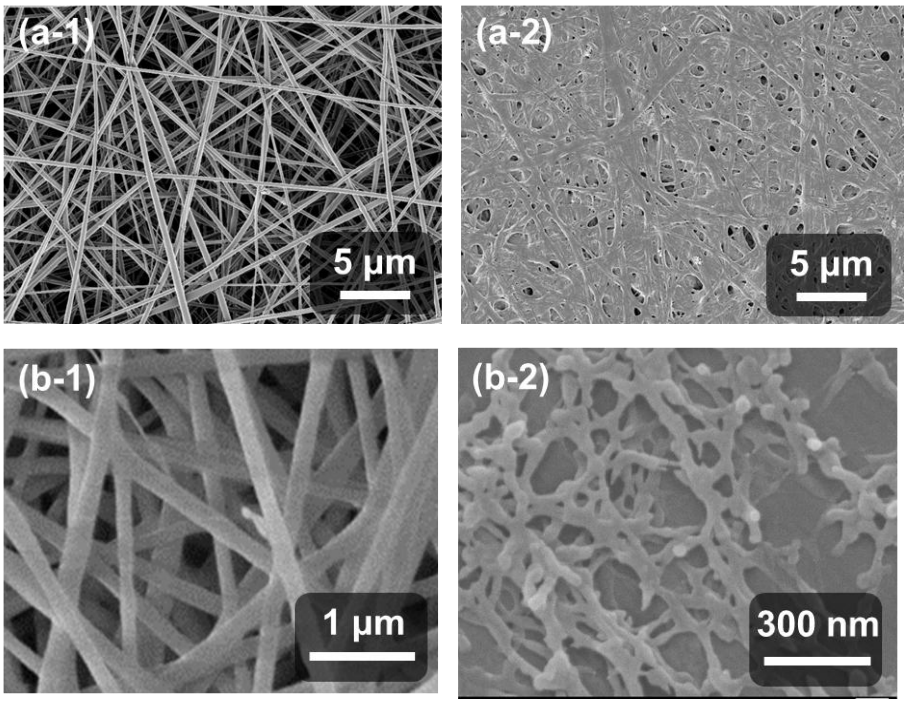

Figure 3.11 Scanning electron micrographs of electrospun fibers before and after removal of auxiliary polymer

(a) MDMO-PPV (b) PCDTBT

3.3 Characterization of optical properties and photoluminescence performance of electrospun P3HT nanofibers

3.3.1 Optical properties of electrospun P3HT nanofiber

Figure 3.12 shows the absorption spectra of electrospun P3HT fibers with a diameter of 80 nm and a spin-coated P3HT film. It is expected that the electric field during electrospinning induces this optical feature of the electrospun P3HT fibers. The P3HT polymer chains are more extended along the applied electric field. It means that the conjugation length is extended, and the crystallinity of the fiber is also increased.

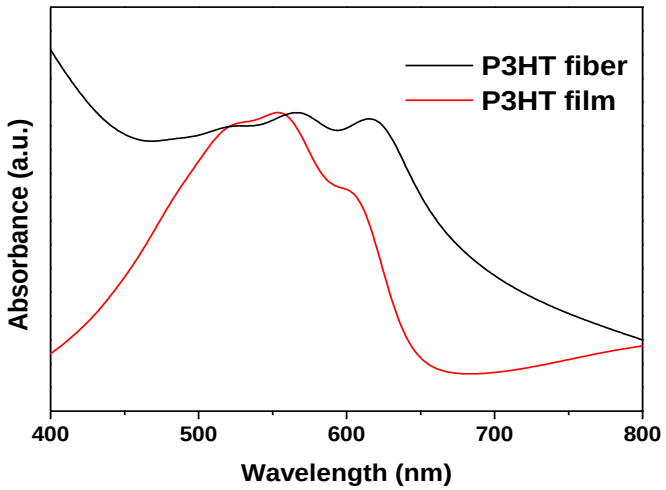

Figure 3.12 UV-visible absorption spectra of virgin P3HT fibers (black solid line) and a P3HT film (red solid line).

As shown in Figure 3.13, an increase in the crystallinity was confirmed by the XRD pattern. For the electrospun P3HT nanofibers, the crystallinity is increased for the (100) surface, as denoted by the 2Θ~5.3 peak. In contrast, for the P3HT film, which was prepared as a reference sample, a peak displaying the (100) surface was not observed. An increase in the conjugation length and the crystallinity of the microstructure of the conjugated polymer allows it to absorb long-wavelength light, thus contributing to better charge transport. Particularly, in contrast to earlier methods, because electrospinning enhances the crystallinity without a heat treatment, it is applicable to flexible boards such as PET.

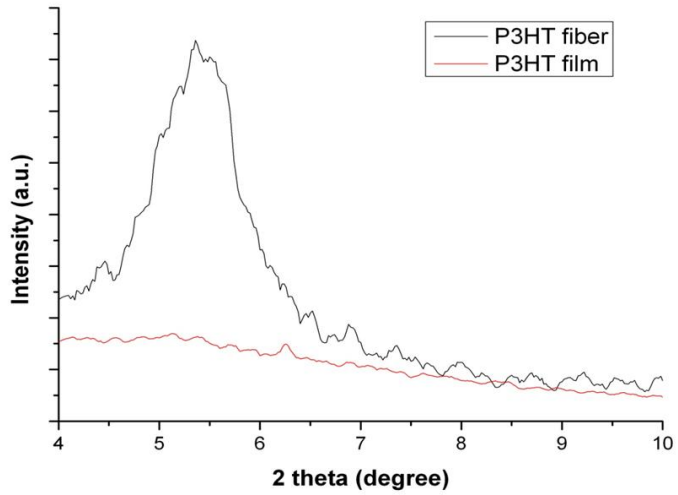

Figure 3.13 XRD patterns of the electrospun P3HT fibers (black solid line) and the spin-cast P3HT film (red solid line) [39].

3.3.2 PL performance of electrospun P3HT nanofiber

To confirm the applicability of electrospun P3HT nanofiber with PEO eliminated to an active layer as a donor material, the PL performance was determined. The PL data achieved are plotted in Figure 3.14. When the donor is blended with an acceptor smoothly, separation of the exciton was noted to occur. A recombination of the separated charge and light emission does not occur. As a result, the PL intensity is decreased. As shown in the figure, as the diameter of the nanofibers is decreased, more effective PL quenching is observed. Particularly at a diameter of 80nm, which is the narrowest in the samples, the result was nearly 100% PL quenching. In other words, by applying nanofibers obtained by this research with a diameter of nearly 80nm, effective exciton dissociation is enabled. Although the diameter of nanofibers is 10~20nm more than the exciton diffusion length, exciton separation was effectively achieved due to the employment of dichloromethane in the PCBM coating. Dichloromethane solves not P3HT but PCBM, serving to swell the P3HT layer, with PCBM permeated into the P3HT layer. In other words, the employment of dichloromethane helps PCBM permeate

into the center of the nanofibers during the coating of PCBM onto the P3HT nanofibers. This effect may enable the formation of an interface between P3HT and PCBM within the exciton diffusion length and may lead to exciton separation efficiency of nearly 100%.

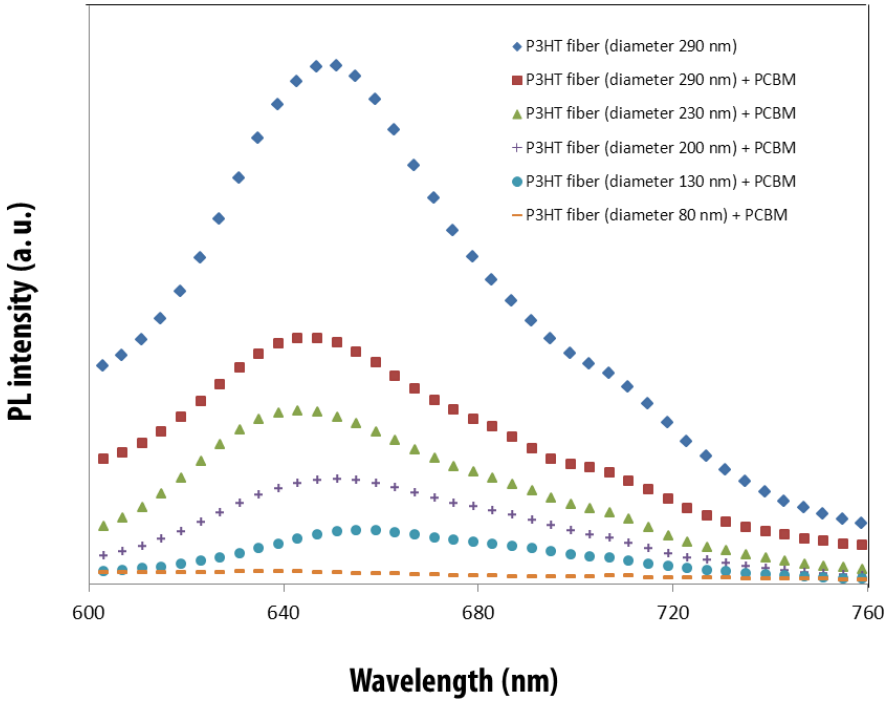

Figure 3.14 PL quenching properties of P3HT nanofibers with various diameters after removal of PEO and PCBM coating.

3.4 Performance of electrospun P3HT nanofiber based OPVs

The OPV cell results for the P3HT nanofiber 80 nm in diameter with the PEO removed are shown in Table 1. In the case of the OPV with the P3HT nanofiber, the structure onto which the nanofiber was coated with PCBM is similar to a bilayer structure. Therefore, to compare the performance of the OPVs, a P3HT : PCBM-bilayer OPV was also characterized.

Though PL quenching implies the effective separation of the exciton, the OPV cell based on the electrospun P3HT nanofiber showed rather low cell efficiency (0.91%). The possible reasons for this low level of efficiency are followed. After the PEO, which acted as an insulator was removed, the PEO residue of about 2~3% remained and thus negative effects were expected. Furthermore, although the exciton separation for the P3HT nanofiber 80nm in diameter was confirmed in the PL result, because the diameter was not thin enough to separate the exciton effectively in the cell, the OPV cell showed lower performance. Finally, the process of fabricating the cell in the laboratory is not optimized, which also may reduce the performance

of the cell. The efficiency and the short circuit current (J_{sc}) of BHJ OPV cells according to the literature are over 3% and 9~11 mA/cm^2, respectively; meanwhile, the same cell fabricated in the laboratory showed efficiency as high as 1.7% and a short circuit current of 7.0 mA/cm^2. In our laboratory, the cell fabrication process, involving the fabrication of an active layer and the deposition of an Al electrode, is not optimized, resulting in poor contact between the layers, which increases the series resistance of the cell.

However, the OPV cell with electrospun P3HT showed values similar to those of a bilayer OPV cell, which has a similar active layer structure. In particular, the short circuit current (J_{sc}) showed a slight increase. Therefore, we expect that the performance of an electrospun P3HT nanofiber-based OPV cell would be improved when the PEO is perfectly removed and the fabrication process of the OPV cell with diameter-controlled nanofibers is optimized.

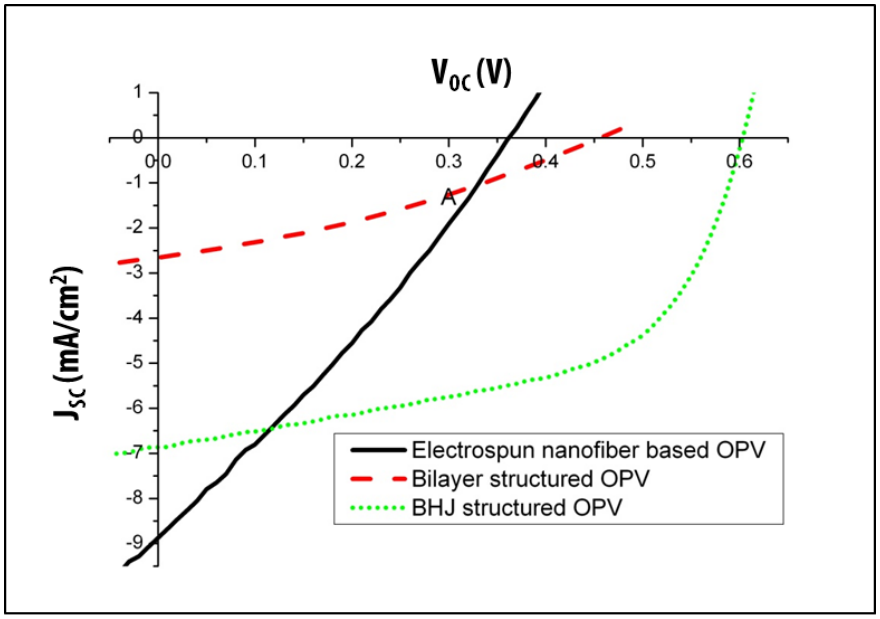

Figure 3.15 Power conversion efficiency of OPV cells with different structures of active layer.

	V_{oc} (V)	J_{sc} (mA/cm^2)	FF	Eff. (%)
Bilayer (P3HT:PCBM)	0.45±0.02	2.4±0.2	0.32±0.04	0.35±0.02
BHJ (P3HT:PCBM)	0.57±0.02	7.0±0.3	0.45±0.02	1.70±0.06
Electrospun P3HT nanofiber	0.37±0.02	8.9±0.2	0.25±0.03	0.91±0.05

Table 3.1 Open circuit voltage (Voc), short circuit current (Jsc), fill factor (FF), power conversion efficiency (η) of OPV cells with different structures of active layer.

4. Conclusion

In this study, P3HT nanofibers 80 nm in diameter with a high aspect ratio were successfully electrospun. For thinner diameters of the nanofibers, the proper amount of PEO as an auxiliary polymer and DMF and acetic acid as a polar solvent were added to the electrospinning dope solution. The addition of DMF increased the viscosity of the electrospun doping solution and the addition of the polar solvent increased the charge density of the electrospun doping solution. The enhanced viscosity and charge density resulted in the fabrication of beadless, thin nanofibers. PEO as an auxiliary polymer played a dominant role in the fabrication of nanofibers but also became an insulation material. After the PEO was removed, the diameter of the P3HT nanofiber was found to be approximately 80 nm. Other conjugated polymers nanofibers were also successfully electrospun. In particular, the diameter of PCD-TBT, a new narrow-bandgap conjugated polymer nanofiber, was found to be 30 nm. To determine the feasibility of the electrospun conjugated polymer nanofiber as donor material for OPVs, electrospun P3HT nanofibers

after the removal of the PEO and PCBM coating was characterized in terms of its photoluminescence (PL). As the diameter of the P3HT nanofibers decreased, the PL intensity became more quenched. In particular, the PL of P3HT nanofiber 80 nm in diameter was found to be quenched at approximately 100 %, indicative of efficient exciton dissociation. This feature is acceptable for OPV cells. When an electrospun P3HT nanofiber-based OPV cell was characterized with I-V measurements, the power conversion efficiency was found to be approximately 1 %. This value was lower than that of a bulk heterojunction structured OPV cell. This result stemmed from the existence of the PEO residue as an insulation material, leading to a greater diameter of the nanofiber than the exciton diffusion length in a non-optimized cell fabrication process. Further research will be devoted to the complete removal of PEO, the preparation of nanofiber with a thinner diameter of less than 20 nm, and the optimization of the cell fabrication process for better performance of electrospun conjugated polymer nanofiber-based OPV cells.

Reference

[1] Spangaard, H. Krebs, *Sol. Energy Mater. Sol. Cells*., 2004, 83, 125.

[2] A. Haugeneder, M. Neges, C. Kallinger, W. Spirkl, *Phys. Rev. B.*, 1999, 59, 15346

[3] D. Vacar, E.S. Maniloff, D. W. McBranch, A. J. Heeger, *Phys. Rev. B.*, 1997, 56, 4573

[4] E. S. Maniloff, V. Klimov, D. McBranch, *Phys. Rev. B.*, 1997, 56, 1876

[5] Watkins, P. K.; Walker, A. B.; Verschoor, G. L. B. Dynamical, *Nano Lett.*, 2005, 5, 1814–1818

[6] Tang, C. W., *Appl. Phys. Lett.*, 1986, *48*, 183.

[7] Rowell, M. W.; Topinka, M. A.; McGehee, M. A.; Prall, H. J.;Dennler, G.; Sariciftci, N. S.; Hu, L.; Gruner, G., *Appl. Phys. Lett.*, 2006, *88*, 233506.

[8] D.M. Basko, E.M. Conwell, *Synth. Met.*, 2003, 139, 819

[9] Breeze, A. J.; Salomon, A.; Ginley, D. S. *Appl. Phys. Lett.*, 2002, *81*, 3085

[10] Yu, G.; Gao, J.; Hummelen, J. C.; Wudl, F.; Heeger, A. J. *Science*, 1995, *270*, 1789.

[11] M. C. Scharber, D. Wuhlbacher, M. Koppe, P. Denk, C. Waldauf, A. J. Heeger and C. L. Brabec, *Adv. Mater.*, 2006, 18, 789–794.

[12] Slota, J. E., He, X., Huck, W. T. S., *Nano Today.*, 2010, 5, 231

[13] Ji Sun Moon, Jae Kwan Lee, Shinuk Cho, Jiyun Byun and Alan J. Heeger *Nano lett*., 2009, 9, 230

[14] A. Laforgue and L. Robitaille, *Synth. Met.*, 2008, 158, 577–584.

[15] C. C. Kuo, C. H. Lin and W. C. Chen, *Macromolecules*, 2007, 40, 6959–6966.

[16] K. M. Coakley, B. S. Srinivasan, J. M. Ziebarth, C. Goh, Y. X. Liu and M. D. McGehee, *Adv. Funct. Mater.*, 2005, 15, 1927–1932.

[17] S. Berson, R. De Bettignies, S. Bailly and S. Guillerez, *Adv. Funct. Mater.*, 2007, 17, 1377–1384.

[18] M. Aryal, K. Trivedi and W. Hu, *ACS Nano*., 2009, 3, 3085–3090

[19] Y. D. Park, H. S. Lee, Y. J. Choi, D. Kwak, J. H. Cho, S. Lee and K. Cho, *Adv. Funct. Mater.*, 2009, 19, 1200–1206.

[20] B.-K. An, S. H. Gihm, J. W. Chung, C. R. Park, S.-K. Kwon and S. Y. Park, *J. Am. Chem. Soc.*, 2009, 131, 3950–3957.

[21] S. M. Jo, M. Y. Song, Y. R. Ahn, C. R. Park and D. Y. Kim, *J. Macromol. Sci., Pure Appl. Chem.*, 2005, 42, 1529–1540.

[22] O. O. Dosunmu, G. G. Chase, W. Kataphinan and D. H. Reneker, *Nanotechnology.*, 2006, 17, 1123–1127.

[23] G. Kim, Y.-S. Cho and W. D. Kim, *Eur. Polym. J.*, 2006, 42, 2031–2038.

[24] G. Taylor, *Proc. R. Soc. London Ser. A.*, 1964, 280, 383 – 397.

[25] S. N. Reznik, A. L. Yarin, A. Theron, E. Zussman, *J. Fluid Mech*., 2004, 516, 349 – 377.

[26] M. Cloupeau, B. Prunet-Foch, *J. Electrost.*, 1989, 22, 135 – 159.

[27] A. L. Yarin, S. Koombhongse, D. H. Reneker, *J. Appl. Phys.*, 2001, 90, 4836 – 4846.

[28] J. W. Andreas Greiner, *Angew. Chem., Int. Ed.*, 2007, 46, 5670–5703.

[29] A. Laforgue and L. Robitaille, *Synth. Met.*, 2008, 158, 577–584.

[30] C. C. Kuo, C. H. Lin and W. C. Chen, *Macromolecules*, 2007, 40, 6959–6966.

[31] D. Li and Y. Xia, *Adv. Mater.*, 2004, 16, 1151–1170.

[32] D. H. Reneker and A. L. Yarin, *Polymer.*,, 2008, 49, 2387–2425.

[33] D. Li, A. Babel, S. A. Jenekhe and Y. Xia, *Adv. Mater.*, 2004, 16, 2062–2066.

[34] A. Babel, D. Li, Y. N. Xia and S. A. Jenekhe, *Macromolecules.*, 2005, 38, 4705–4711.

[35] Rosana González, Nicholas J. Pinto, *Synth Met.*, 2005;151:275

[36] Alexis Laforgue, Lucie Robitaille, *Synth Met.*, 2008;158:577

[37] Kezhen Yin, Lifeng Zhang, Chuilin Lai, Lanlan Zhong, Steve Smith, Hao Fong and Zhengtao Zhu, *J. Mater. Chem.*, 2011, 21, 444

[38] Sungwon Lee, Geon Dae Moon and Unyong Jeong, *J. Mater. Chem.*, 2009, 19, 743

[39] Taehoon Kim, J. H. Im, H. S. Choi, S. J. Yang, S. W. Kim and C.R. Park *J. Mater. Chem.*, 2011, 21, 14231

초 록

태양전지는 빛을 흡수하여, 전력을 생산하는 기기로, 전하를 수집하는 전극과 생성하는 광활성층으로 이루어져 있다. 광활성층이 유기 물질로 된 경우, 유기 태양전지라 하며, 일반적으로 전자 주개 물질과 전자 받개 물질을 잘 섞어, 벌크 이종접합 구조의 광활성층을 사용한다. 벌크 이종접합 구조는, 이중층 구조에 비해 전자 주개 물질과 받개 물질 간의 계면을 크게 증가시킬 수 있고, 이에 따라 엑시톤의 분리가 더 효과적으로 일어날 수 있다. 하지만, 전자 주개 물질과 받개 물질이 서로 뒤섞여 광활성층을 형성하기 때문에, 중간중간 독립된 상을 만들게 된다. 이러한 상에서는, 분리된 전하가 전극으로 이동할 수 없고, 재결합하여 에너지를 방출하게 된다. 따라서, 전하 수송을 원활히 하기 위해, 광활성층에 하나로 이어진 전하 이동 통로가 형성되어야 한다. 이와 관련하여, 1-D 구조 공액 고분자는, 지름 대비 길이 비율이 크기 때문에, 전하 이동 통로를 형성하기에 적합하다. 전기방사는 대부분의 고분자를 이용하여 1-D 구조의 나노섬유를 만들 수 있는, 간편한 방법이다. 본 연구에서는, 전기방사를 통해 가장 대표적인 전자 주개 물질인 P3HT 를, 얇은 지름의 나노섬유로

제조하고, 이를 유기 태양전지 광활성층으로서 적용가능성을 확인해 보고자 한다. 더 얇은 지름으로 조절하기 위해, 전기방사용액에 보조 고분자인 PEO 와 극성 용매인 DMF, acetic acid 를 적정량 첨가하였다. PEO 첨가로 전기방사용액의 점성을, 극성 용매 첨가로 전기전도도를 적정 수준으로 증가시켰다. 개선된 점성과 전기전도도로 인해, 뭉침 현상 없이 얇은 나노섬유를 제조하였다. 부도체인, PEO 를 제거한 이후, 80 nm의 얇은 지름을 갖는 P3HT 나노섬유를 형성하였다. 특히, 새로운 전자 주개 물질 중 하나인, PCDTBT 나노섬유의 지름은 30 nm 로 조절되었다. PL quenching 현상을 통하여 제조된 P3HT 나노섬유에서 엑시톤 분리가 효과적으로 일어나고 있음을 확인하였고, 이를 광활성층으로 적용하여 1 %의 효율을 갖는 태양 전지 셀을 만들 수 있었다. 추후, 최적화 공정을 통하여 셀 효율을 상승시킬 수 있을 것이라 기대된다.

주요어: 유기 태양 전지, 공액 고분자, 전기 방사, 나노 섬유, 엑시톤 분리

학 번: 2010-20581